Supplementary Information for:

# A reactive Ru-binaphtholate building block with self-tuning hapticity

*Johanna M. Blacquiere, Carolyn S. Higman, Robert McDonald[†] and Deryn E. Fogg**

Center for Catalysis Research & Innovation, and Department of Chemistry, University of Ottawa, Ottawa ON, Canada K1N 6N5

**Table of Contents:**



[†] X-Ray Crystallography Laboratory, Chemistry Department, University of Alberta, 11227 Saskatchewan Drive NW, Edmonton AB, Canada T6G 2G2.

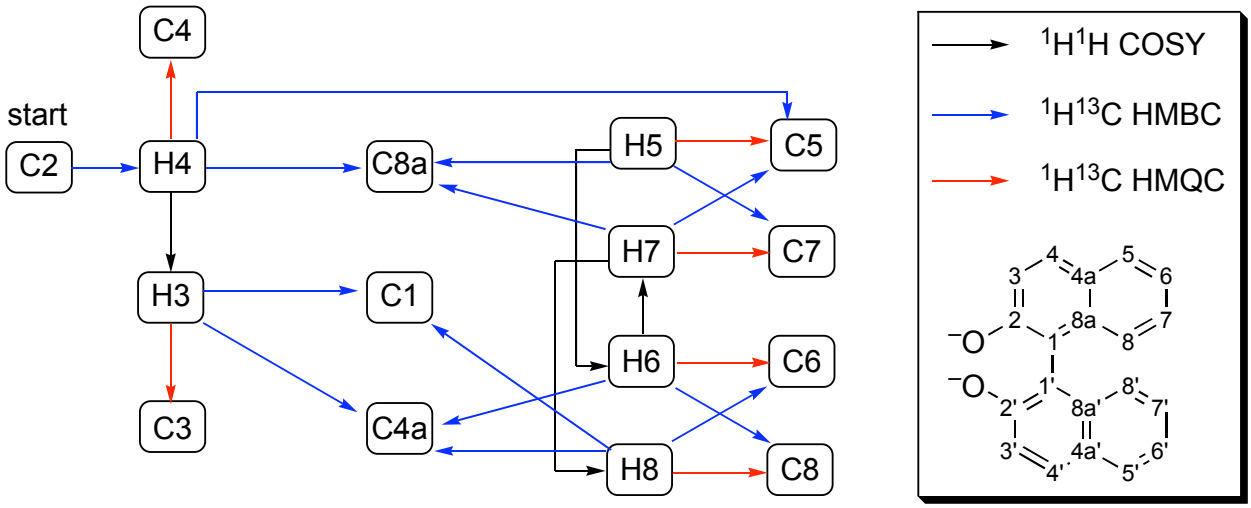


**Figure S1.** Road map showing a convenient strategy for assignment of key $^1$H and $^{13}$C NMR signals for the BINO ligand. (Black arrows: $^1$H-$^1$H COSY; blue, $^1$H-$^{13}$C HMBC; red: $^1$H-$^{13}$C HMQC).

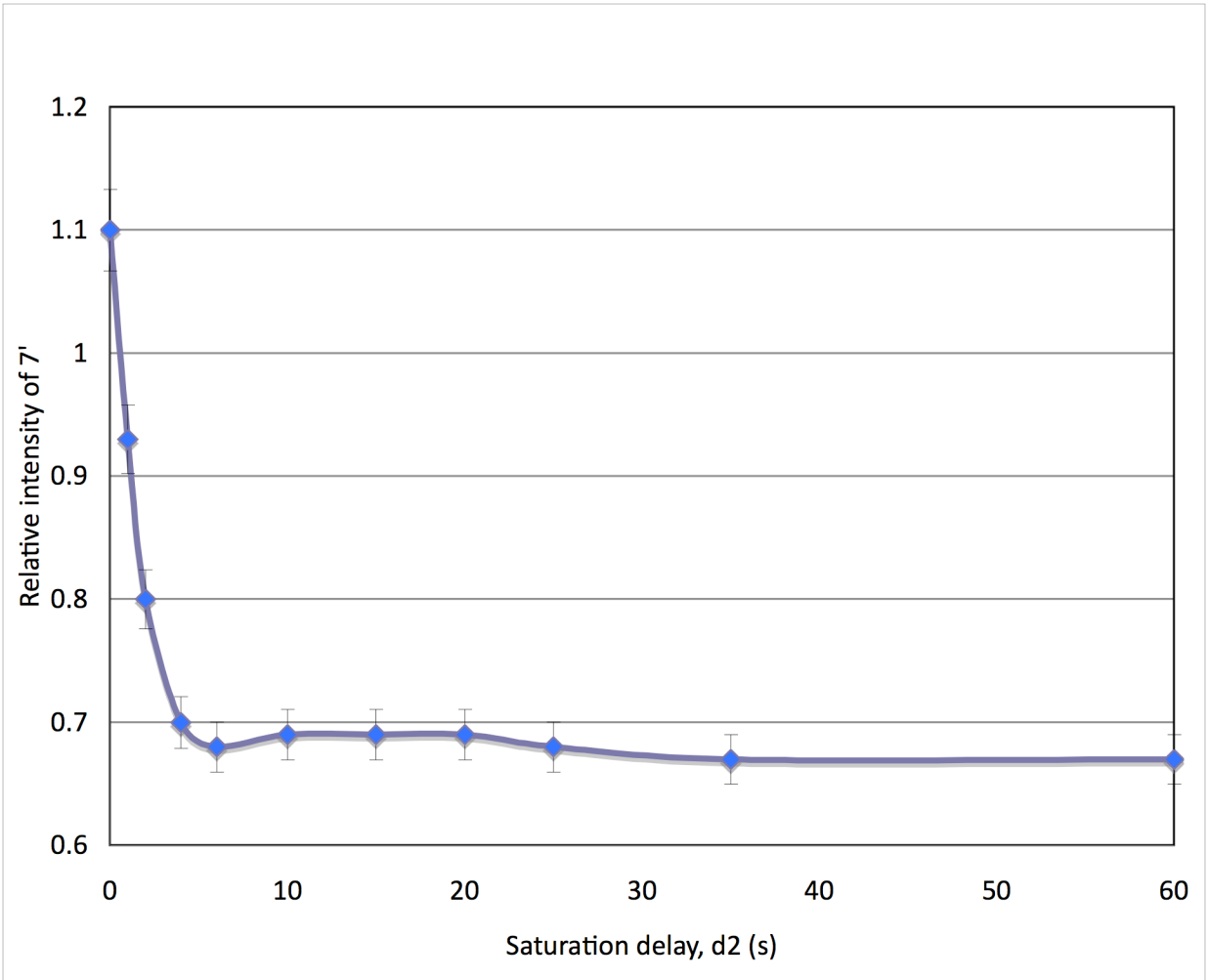


**Figure S2.** $^{31}$P spin saturation transfer plot: relative intensities of the signal for **7'** after saturating that for **7"**, as a function of the saturation delay (40 °C, $C_6D_6$).

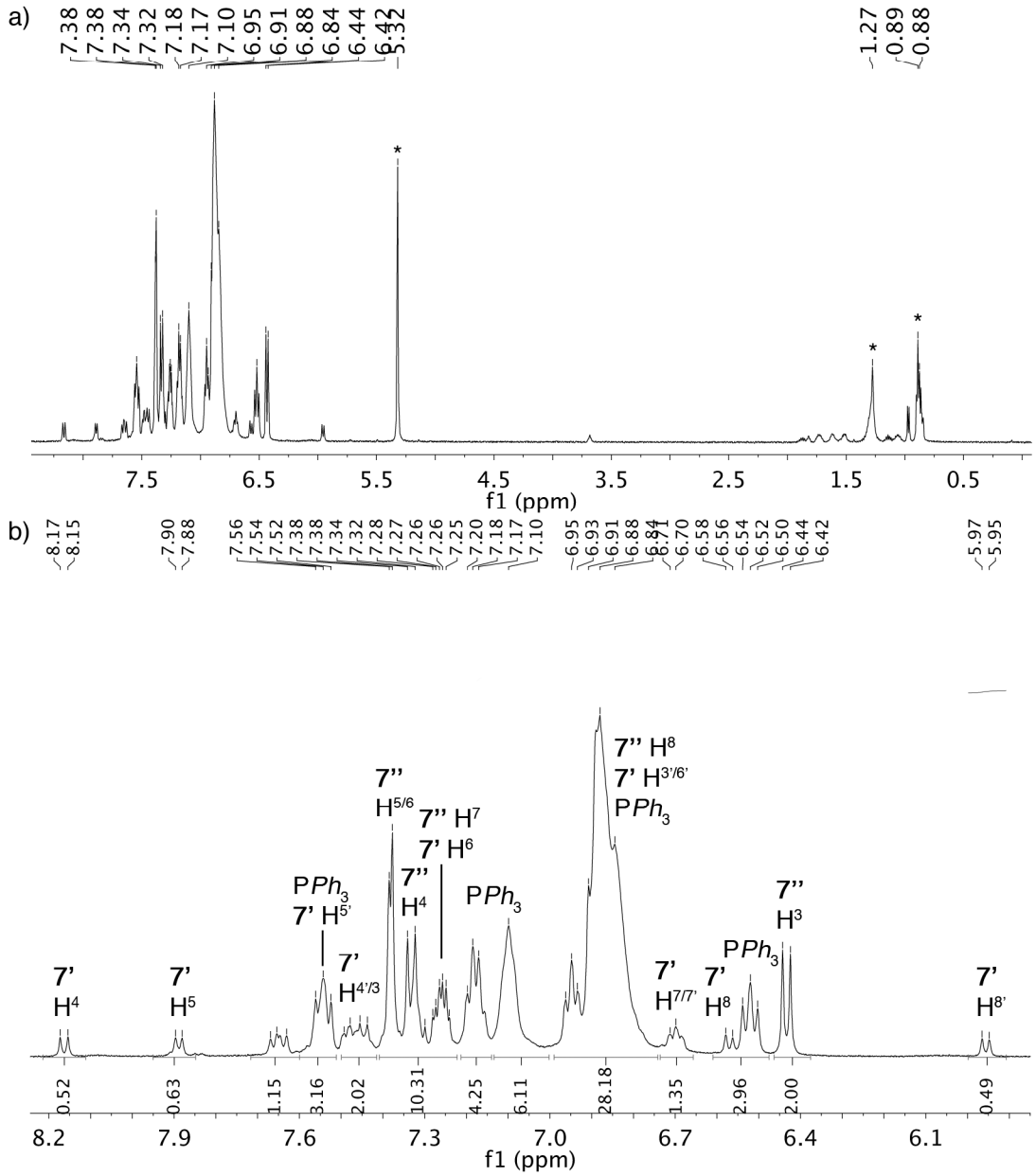


**Figure S3.** $^{1}$H NMR spectrum of **7** ($CD_2Cl_2$). (a) Full spectrum; (b) expansion of the aromatic region with peak assignments. Solvent peaks are designated by (*).

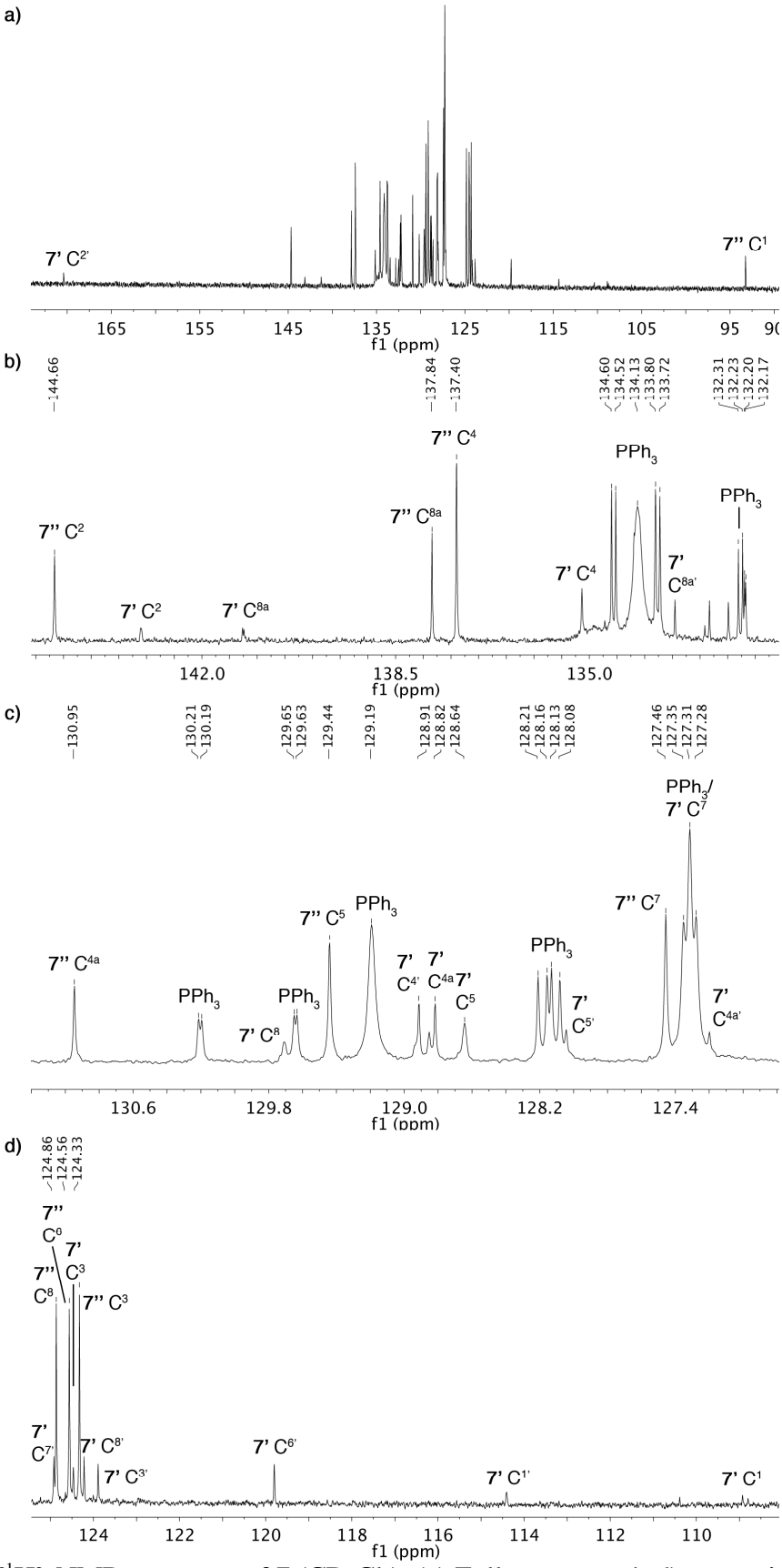


**Figure S4.** $^{13}C\{^{1}H\}$ NMR spectrum of **7** ($CD_2Cl_2$). (a) Full spectrum; b-d) expansions of the aromatic region with peak assignments.

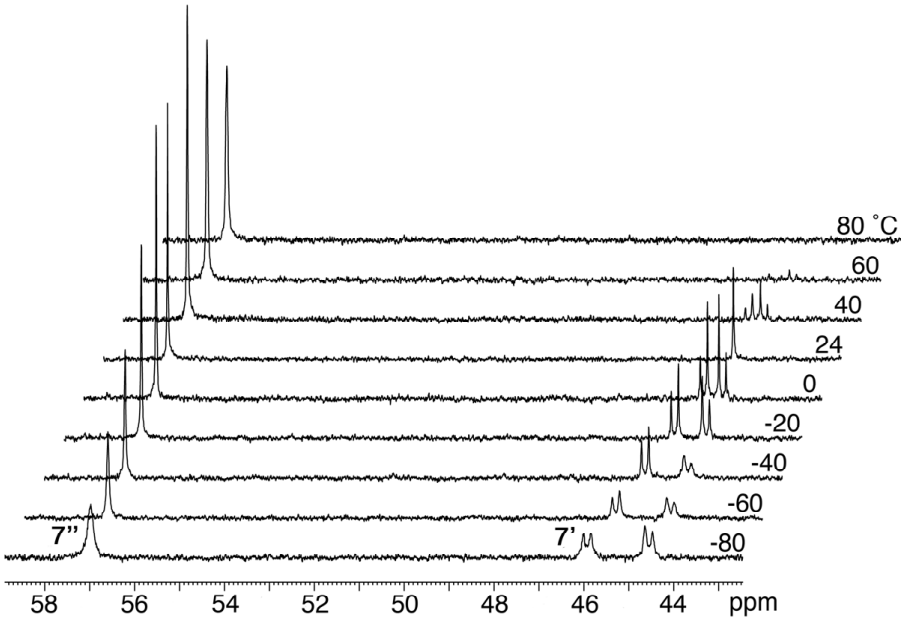


**Figure S5.** Variable-temperature $^{31}P\{^{1}H\}$ NMR spectra of **7** ($CD_2Cl_2$). At 24 ˚C, **7"** appears at 56.9 ppm, **7'** at 43.5 ppm.

**Table S1.** Proportions of **7"** and **7'** in common solvents.[a]

| Solvent | Relative % | |
|---|---|---|
| | **7''** | **7'** |
| $CDCl_3$ | 100 | 0 |
| $CD_2Cl_2$ | 79 | 21 |
| $C_7D_8$ | 73 | 27 |
| $C_6D_6$ | 67 | 33 |
| THF | 53 | 47 |
| THF[b] | 54 | 46 |

[a] Determined from relative $^{31}P\{^{1}H\}$ NMR integration values. [b] After 5 h in solution.

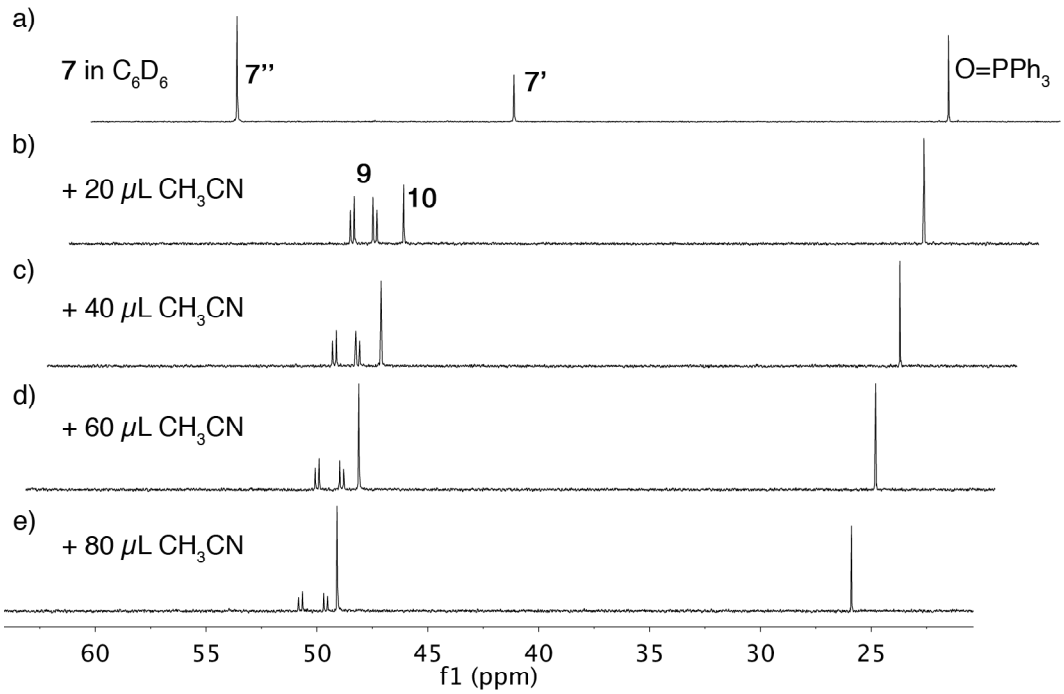


**Figure S6.** $^{31}P\{^{1}H\}$ NMR spectra showing transformation of **7** ($C_6D_6$) into **9** and **10** on addition of MeCN. Ratios of **9**:**10** as a function of added $CH_3CN$ are as follows: (b) 3:1; (c) 1.1:1; (d) 1:1.3; (e) 1:2. $OPPh_3$ used as internal standard.

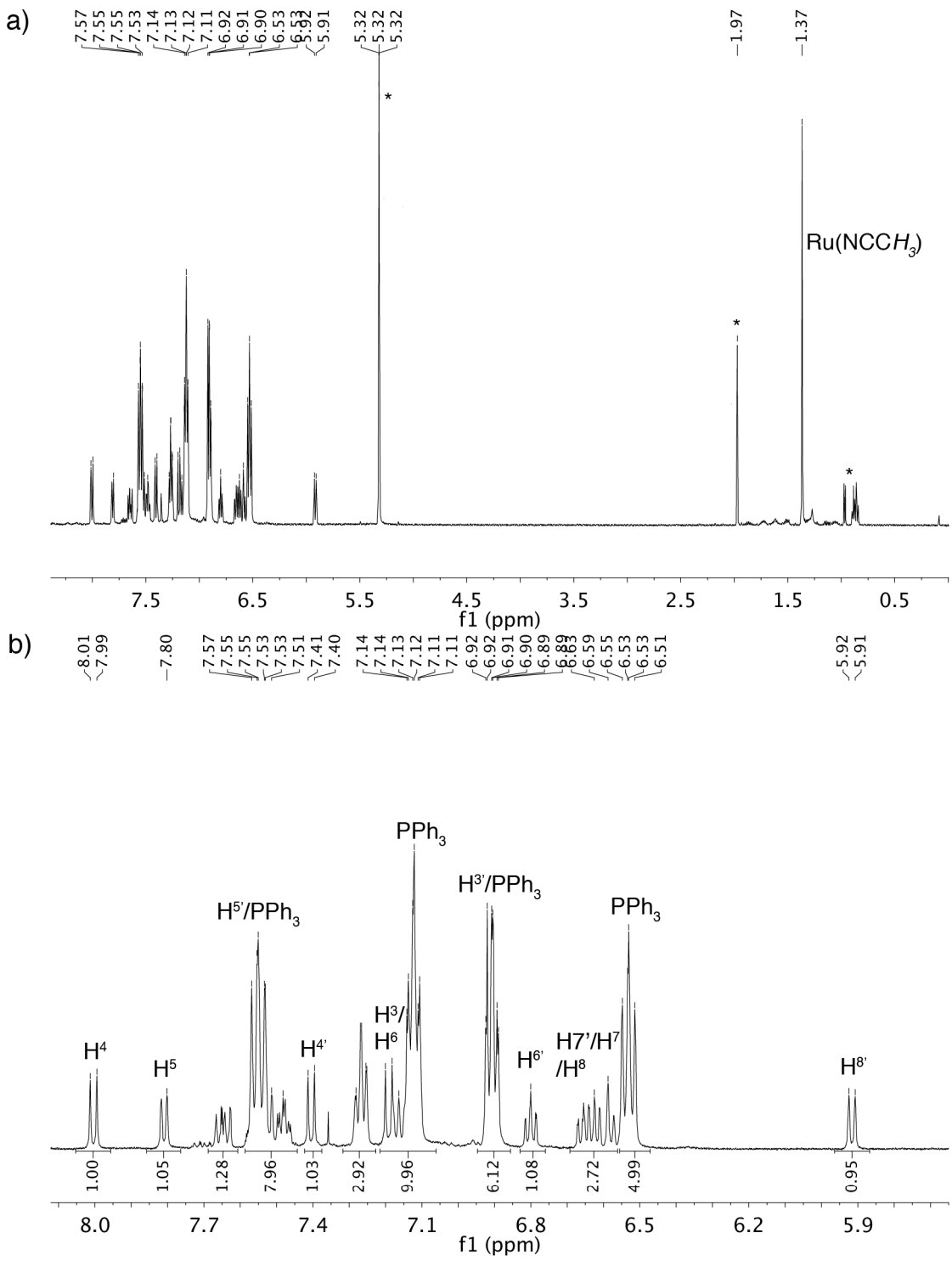


**Figure S7.** $^{1}$H NMR spectrum of **9** ($CD_2Cl_2$). (a) Full spectrum; (b) expansion of the aromatic region with peak assignments. Solvent peaks are designated by (*).

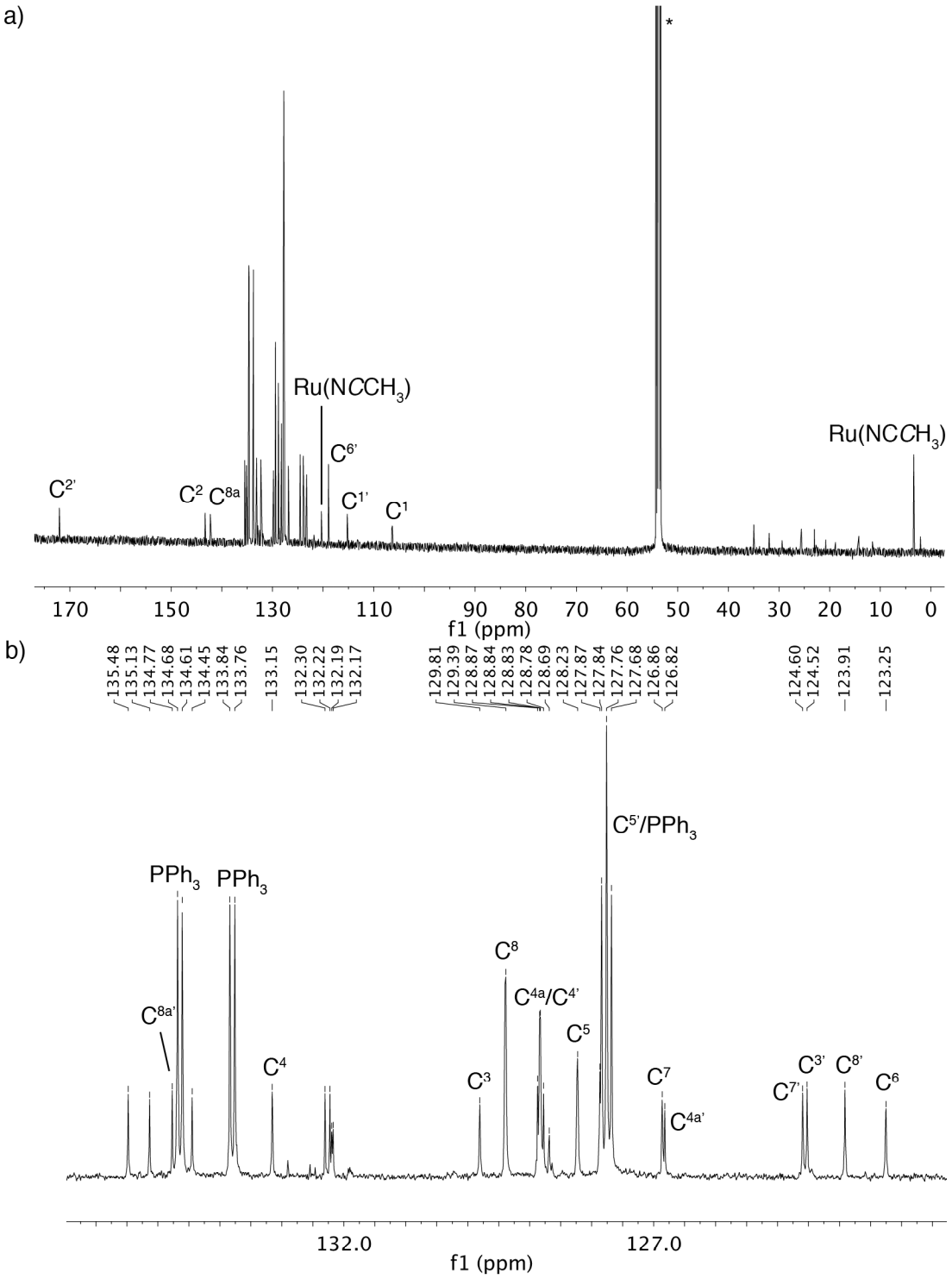


**Figure S8.** $^{13}C\{^{1}H\}$ NMR spectrum of **9** ($CD_2Cl_2$). (a) Full spectrum; (b) expansion of the aromatic region, showing peak assignments. Unassigned signals are due to $OPPh_3$; residual solvent signals are designated (*).

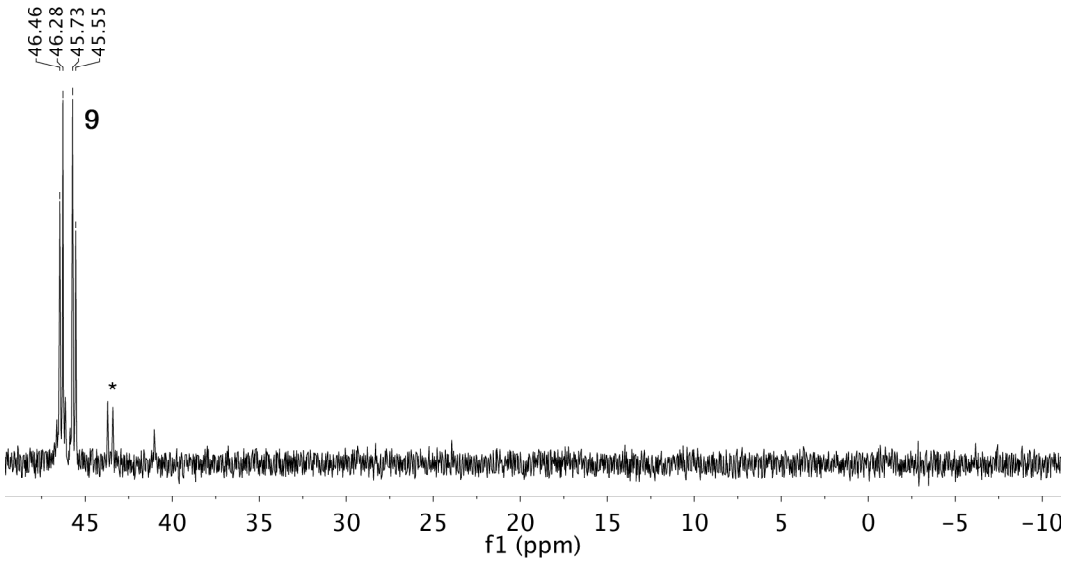


**Figure S9.** $^{31}P\{^{1}H\}$ NMR spectrum of **9** ($CD_2Cl_2$). Unassigned signals are designated by (*).

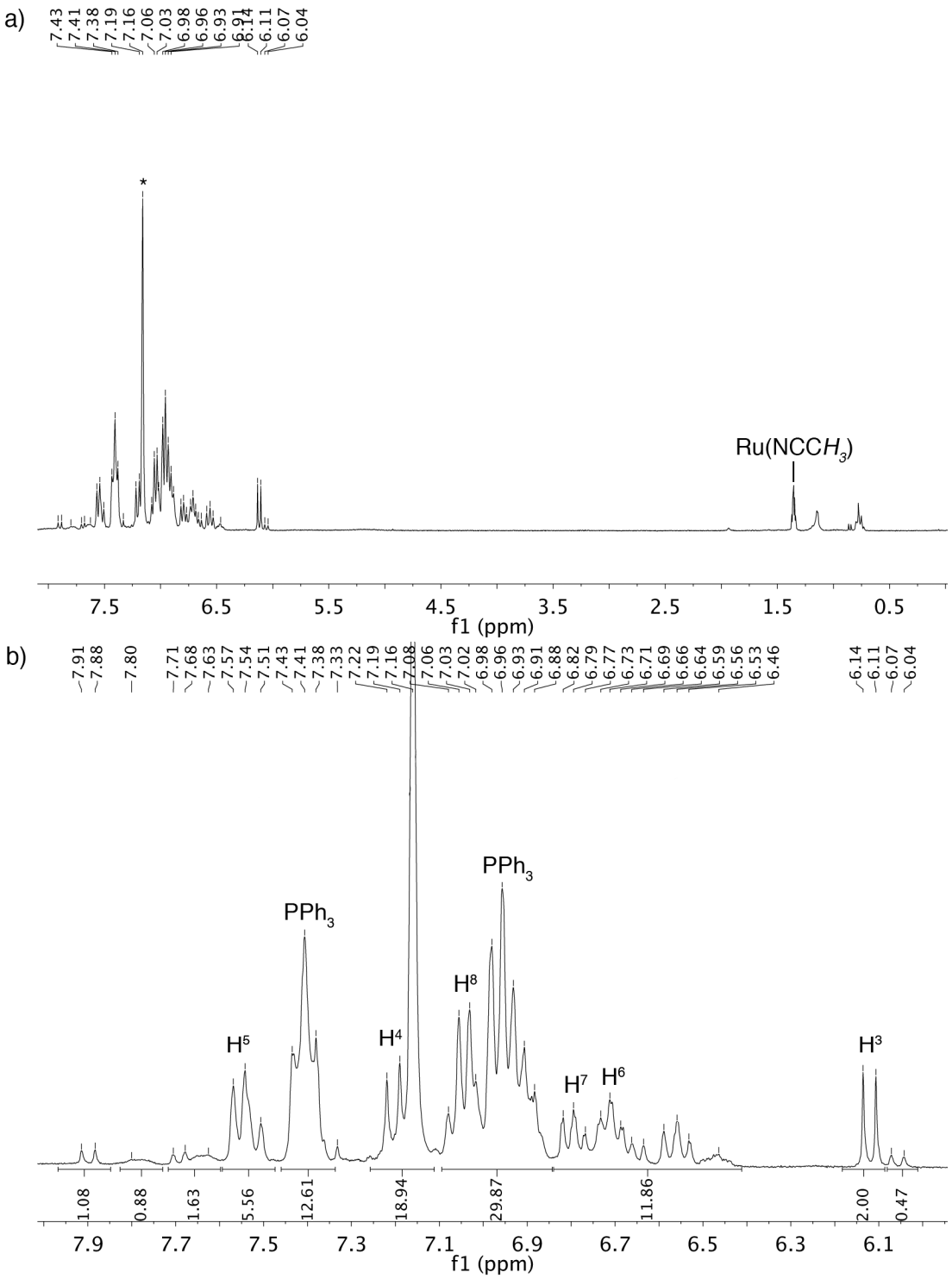


**Figure S10.** $^{1}$H NMR spectrum of **10** (1:2 $CD_3CN$-$C_6D_6$). (a) Full spectrum; (b) expansion of the aromatic region with peak assignments. Complex **9** (ca. 10%) is also present. Solvent peaks are designated by (*).

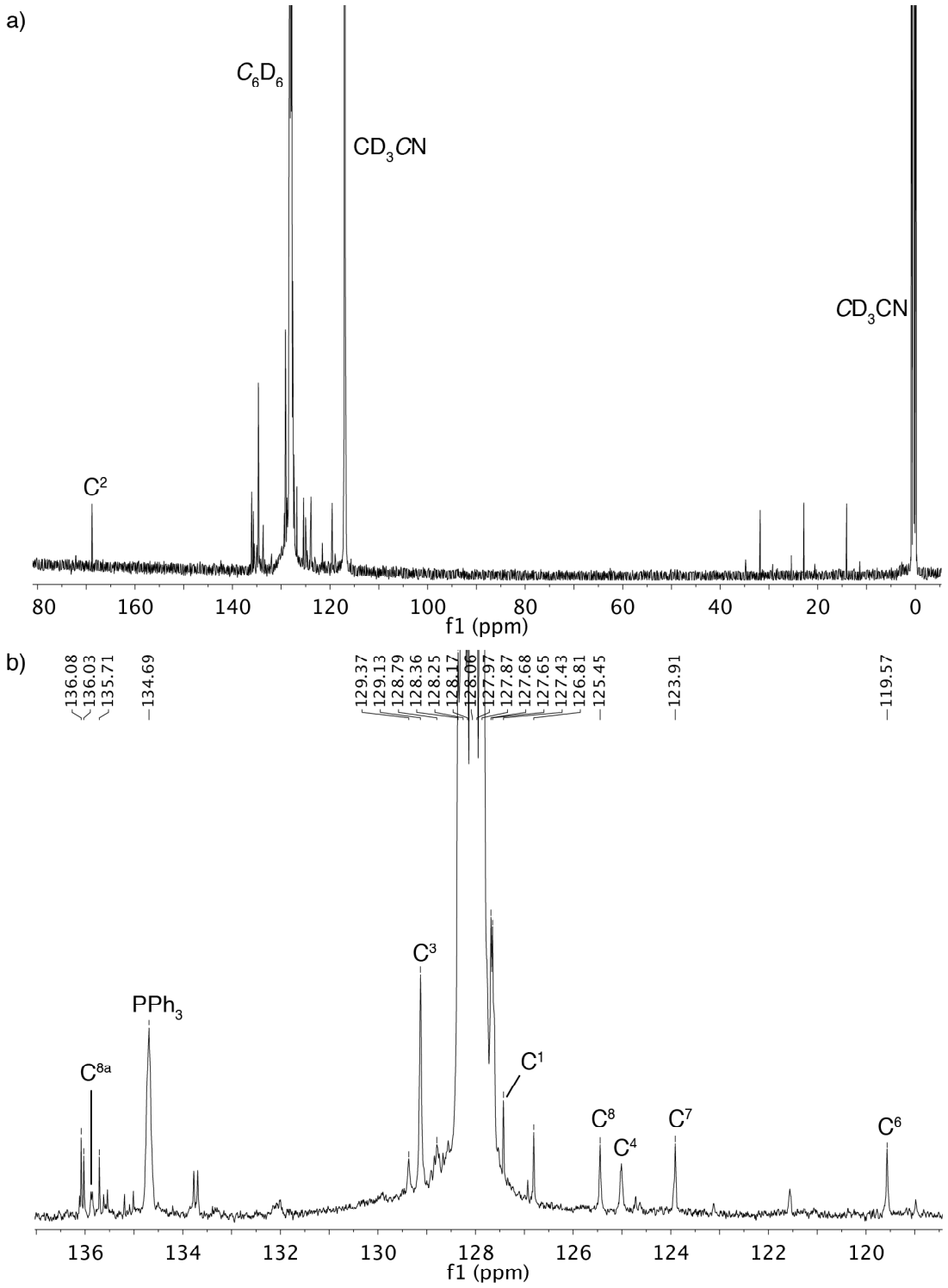


**Figure S11.** $^{13}C\{^1H\}$ NMR spectrum of **10** (1:2 $CD_3CN$-$C_6D_6$). (a) Full spectrum; (b) expansion of the aromatic region with peak assignments. The $C_6D_6$ solvent signal obscures peaks for $PPh_3$, C4a and C5; their locations were determined by correlation experiments.

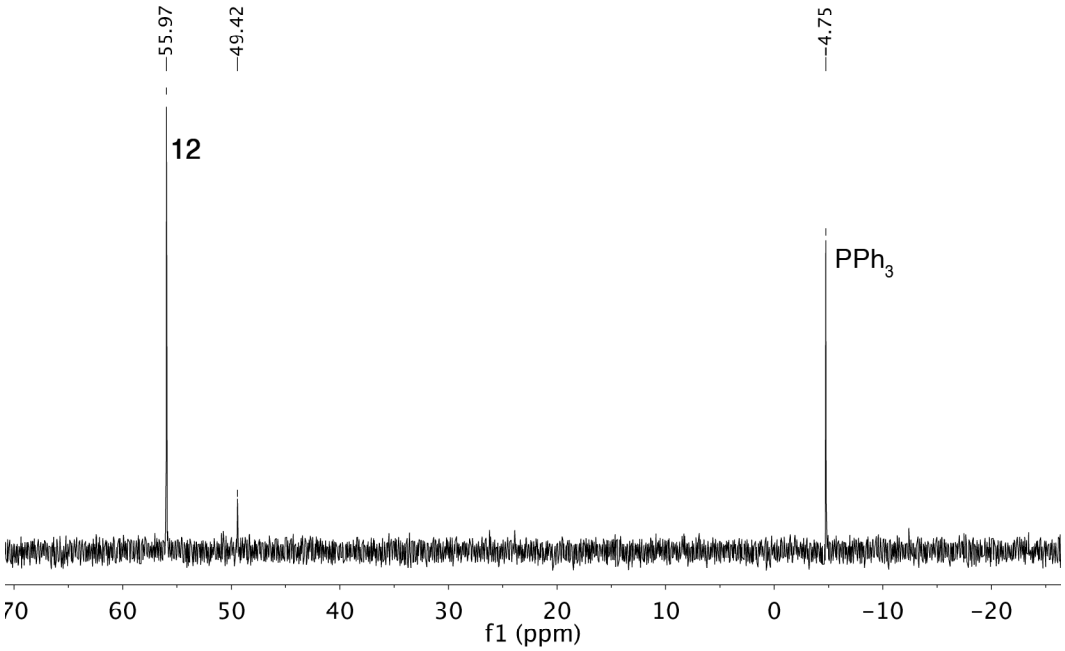


**Figure S12.** $^{31}P\{^{1}H\}$ NMR spectrum revealing the in situ formation of **12** and free $PPh_3$ on adding pyridine to **7** ($C_5H_5N$ with $C_6D_6$ for lock). The signal at 49.4 ppm is an unidentified side-product.

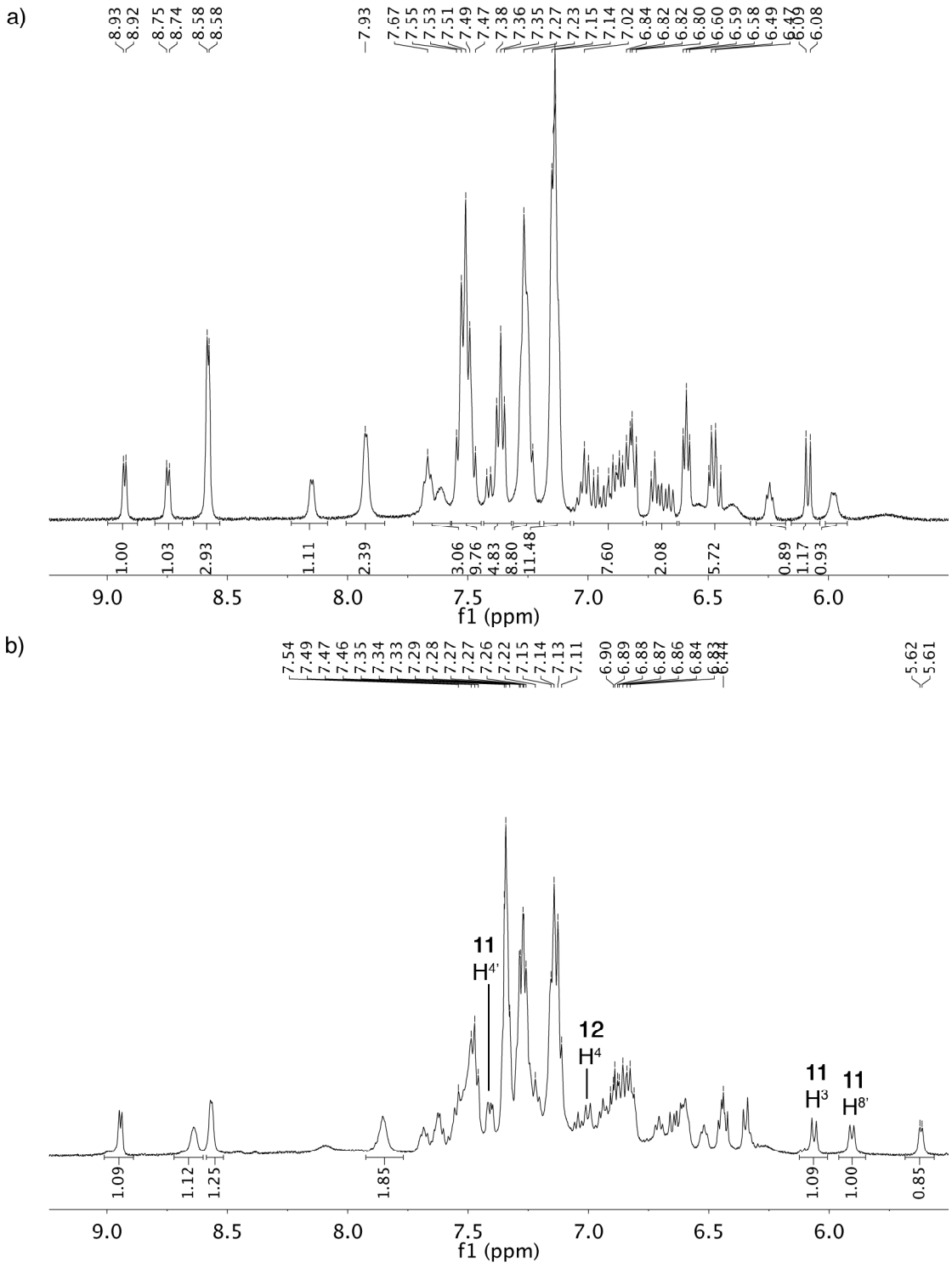


**Figure S13.** $^1$H NMR spectrum of the **11**-**12** mixture (20% **12**; $CD_2Cl_2$). (a) Aromatic region at 24 ˚C; (b) aromatic region at –20 ˚C. Assignments are included for resonances located via correlation experiments.

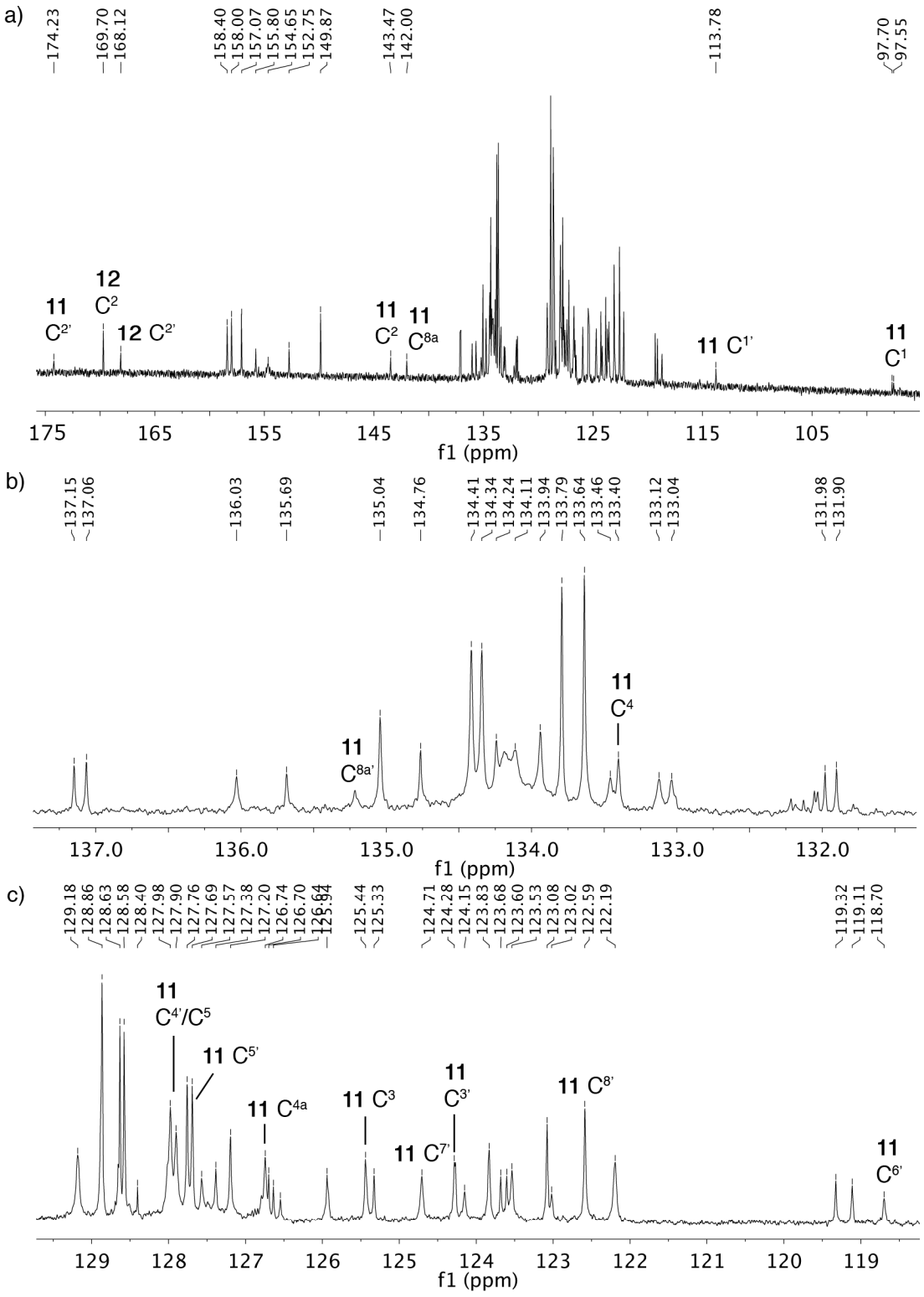


**Figure S14.** Low-temperature $^{13}C\{^1H\}$ NMR spectrum of the **11**-**12** mixture (20% **12**; $CD_2Cl_2$; –20 ˚C). (a) Aromatic region; b and (c) expansions of the aromatic region. Assignments are included for resonances located via correlation experiments.

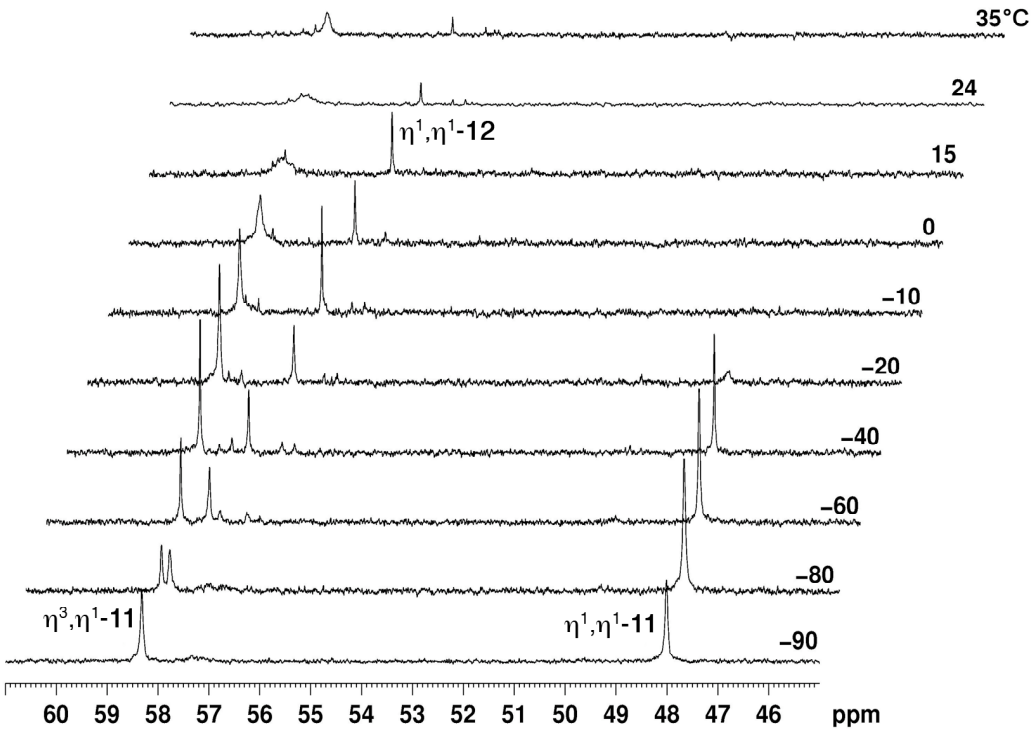


**Figure S15.** Variable-temperature $^{31}P\{^{1}H\}$ NMR spectra of the **11**-**12** mixture (20% **12**; $CD_2Cl_2$).

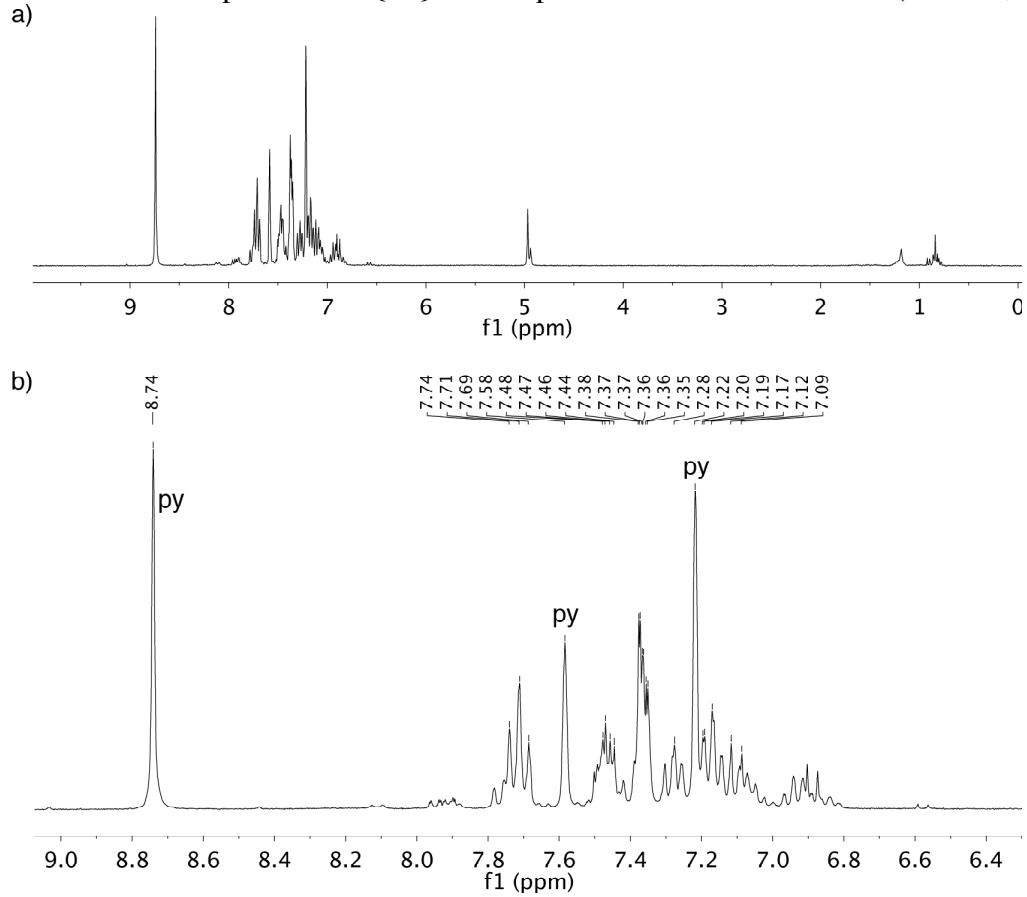


**Figure S16.** $^{1}H$ NMR spectrum of **12** in $C_5D_5N$. (a) Aromatic region; (b) expansion of the aromatic region.

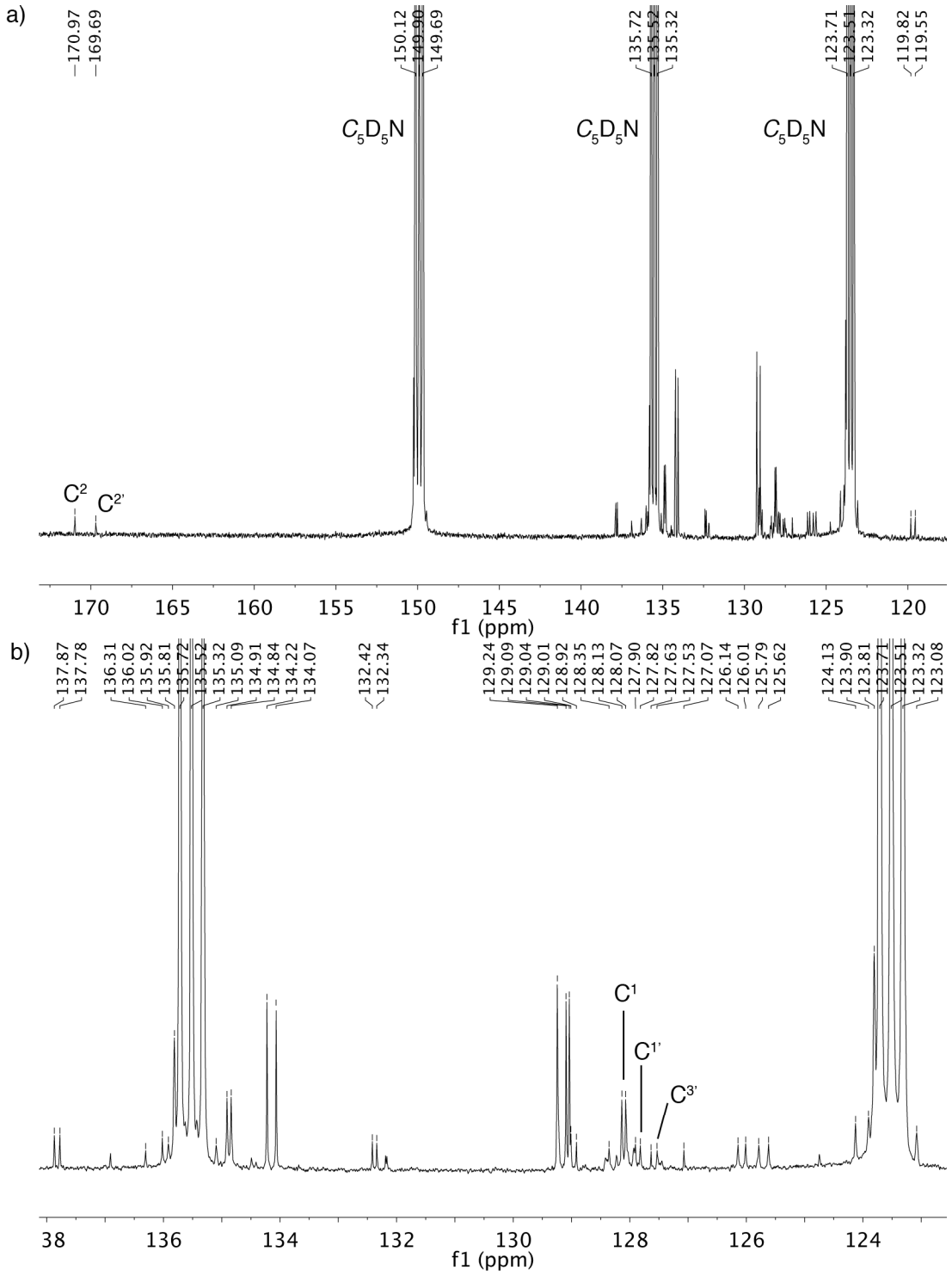


**Figure S17.** $^{13}C\{^{1}H\}$ NMR spectrum of **12**, obtained by dissolving **11** in $C_5D_5N$. (a) Aromatic region; (b) expansion of the aromatic region. Assignments are included for signals located via correlation experiments.

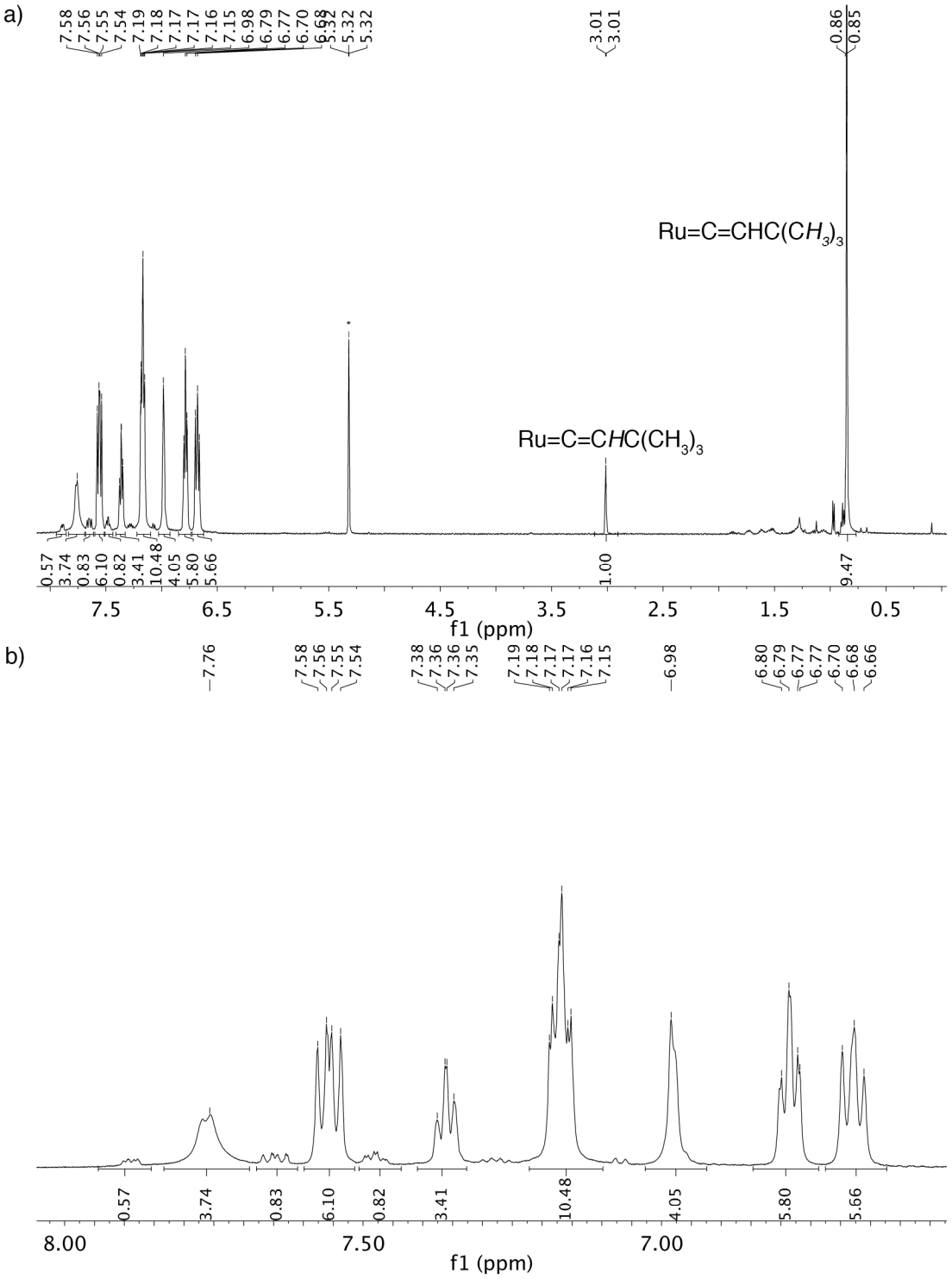


**Figure S18.** $^{1}$H NMR spectrum of **13** ($CD_2Cl_2$) acquired at 24 ˚C. (a) Full spectrum; (b) expansion of the aromatic region. Solvent peaks are designated by (*).

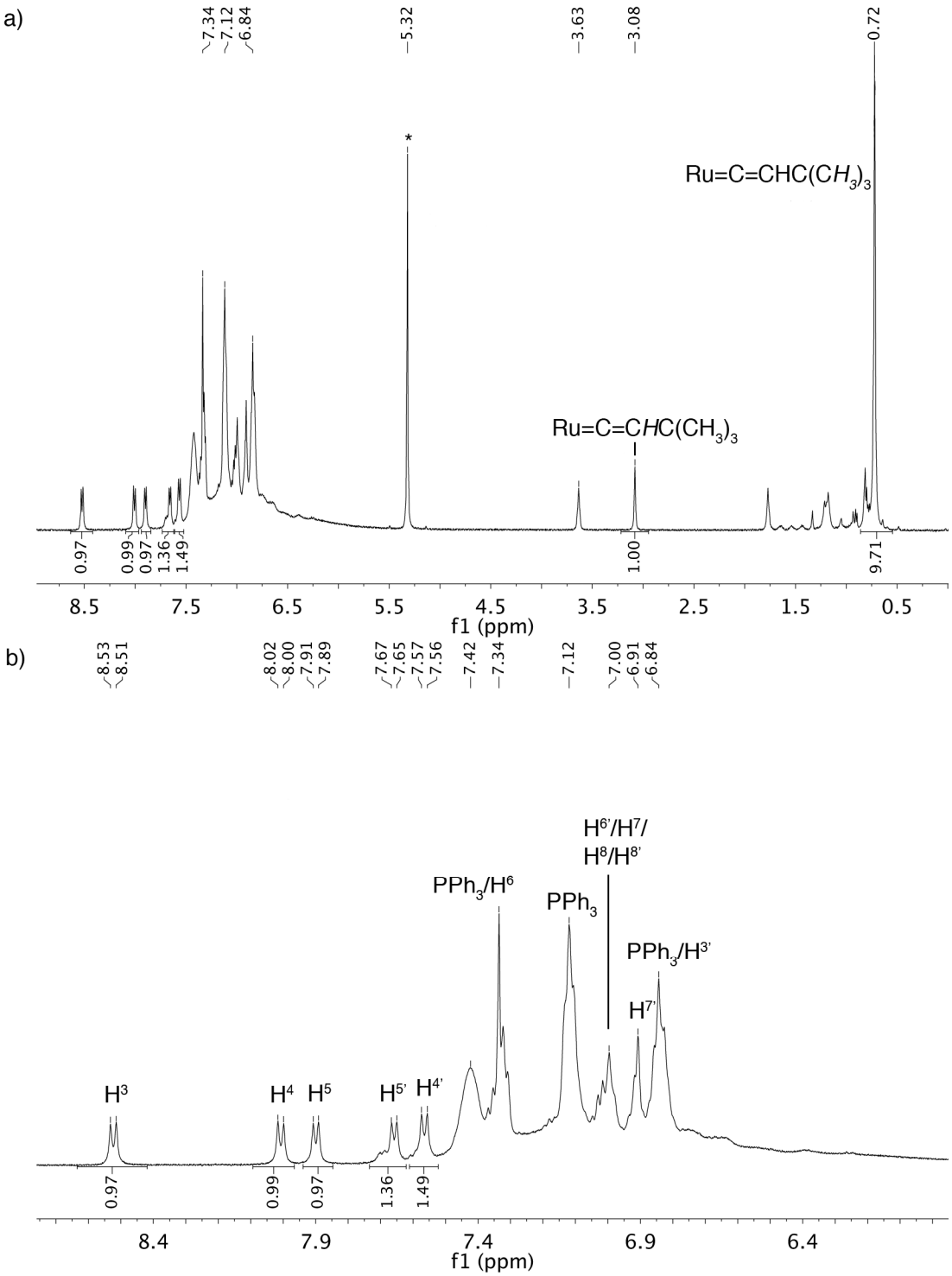


**Figure S19.** Low-temperature $^{1}$H NMR spectrum of **13** ($CD_2Cl_2$, –60 °C). (a) Full spectrum; (b) expansion of the aromatic region. Solvent peaks are designated by (*).

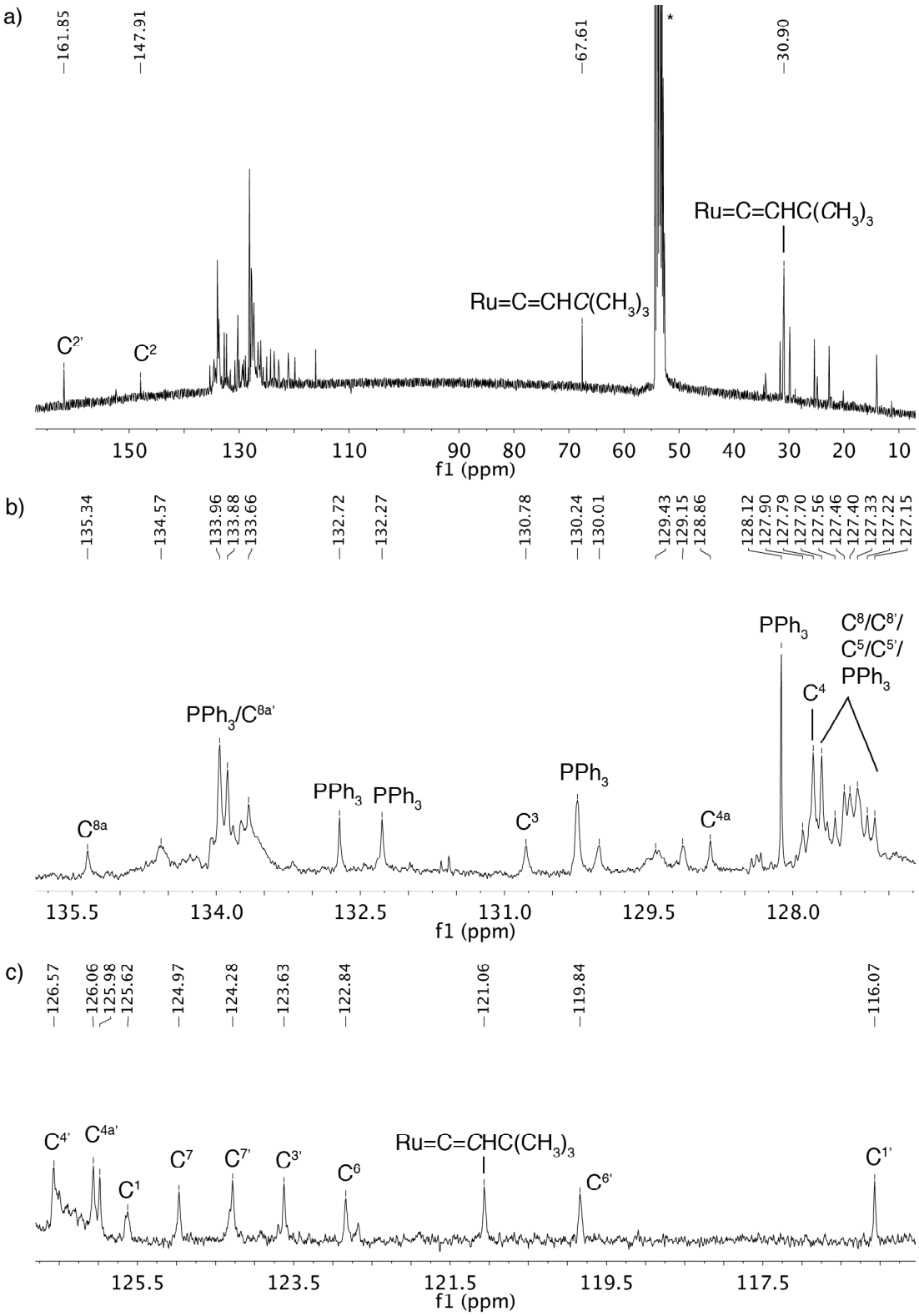


**Figure S20.** $^{13}C\{^{1}H\}$ NMR spectrum of **13** ($CD_2Cl_2$) acquired at –60 ˚C. (a) Full spectrum; (b) and (c), expansions of the aromatic region with signal assignments. The Ru*C* signal (δ = 347.2 ppm) is not shown: it was located via a $^{1}H$-$^{13}C$ HMBC correlation experiment. Solvent peaks are designated by (*).

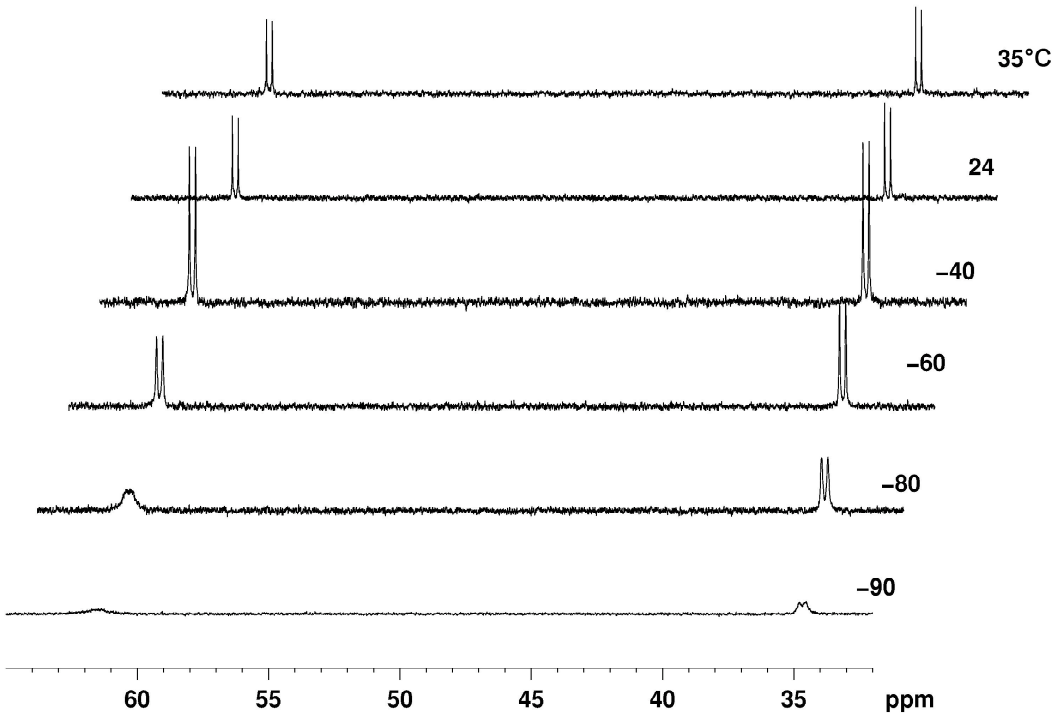


**Figure S21.** Variable-temperature $^{31}P\{^{1}H\}$ NMR spectra of **13** ($CD_2Cl_2$). Signal broadening at low temperatures may reflect isomerization from $\eta^3,\eta^1$- to $\eta^1,\eta^1$-BINO coordination.